Water Resources Research

RESEARCH ARTICLE
10.1029/2017WR021719

Key Points:
- Mobile Cosmic-Ray Neutron Sensing can capture small-scale patterns of root-zone soil water at scales from tens to hundreds of meters
- Neutron simulations and field experiments reveal that CRNS estimation of field soil moisture is substantially biased by the presence of roads
- We propose a practical correction approach that is essential to provide unbiased soil water data for hydrological applications

Supporting Information:
- Supporting Information S1

Correspondence to:
M. Schrön,
martin.schroen@ufz.de

Citation:
Schrön, M., Rosolem, R., Köhli, M., Piussi, L., Schröter, I., Iwema, J., et al. (2018). Cosmic-ray neutron rover surveys of field soil moisture and the influence of roads. *Water Resources Research*, *54*, 6441–6459. https://doi.org/10.1029/2017WR021719

Received 28 OCT 2017
Accepted 27 JUN 2018
Accepted article online 12 MAY 2018
Published online 15 SEP 2018

Cosmic-ray Neutron Rover Surveys of Field Soil Moisture and the Influence of Roads

M. Schrön[1,2], R. Rosolem[2,3], M. Köhli[1,4,5], L. Piussi[6], I. Schröter[1], J. Iwema[2], S. Kögler[1], S. E. Oswald[7], U. Wollschläger[8], L. Samaniego[9], P. Dietrich[1], and S. Zacharias[1]

[1]Department of Monitoring and Exploration Technologies, Helmholtz Centre for Environmental Research - UFZ, Leipzig, Germany, [2]Faculty of Engineering, University of Bristol, Bristol, UK, [3]Cabot Institute, University of Bristol, Bristol, UK, [4]Physikalisches Institut, Heidelberg University, Heidelberg, Germany, [5]Physikalisches Institut, University of Bonn, Bonn, Germany, [6]Faculty of Science and Technology, Free University of Bolzano-Bozen, Bozen, Italy, [7]Institute of Earth and Environmental Science, University of Potsdam, Potsdam, Germany, [8]Department for Soil Physics, Helmholtz Centre for Environmental Research - UFZ, Halle (Saale), Germany, [9]Department of Computational Hydrosystems, Helmholtz Centre for Environmental Research - UFZ, Leipzig, Germany

Abstract Measurements of root-zone soil moisture across spatial scales of tens to thousands of meters have been a challenge for many decades. The mobile application of Cosmic Ray Neutron Sensing (CRNS) is a promising approach to measure field soil moisture noninvasively by surveying large regions with a ground-based vehicle. Recently, concerns have been raised about a potentially biasing influence of local structures and roads. We employed neutron transport simulations and dedicated experiments to quantify the influence of different road types on the CRNS measurement. We found that roads introduce a substantial bias in the CRNS estimation of field soil moisture compared to off-road scenarios. However, this effect becomes insignificant at distances beyond a few meters from the road. Neutron measurements on the road could overestimate the field value by up to 40 % depending on road material, width, and the surrounding field water content. The bias could be largely removed with an analytical correction function that accounts for these parameters. Additionally, an empirical approach is proposed that can be used without prior knowledge of field soil moisture. Tests at different study sites demonstrated good agreement between road-effect corrected measurements and field soil moisture observations. However, if knowledge about the road characteristics is missing, measurements on the road could substantially reduce the accuracy of this method. Our results constitute a practical advancement of the mobile CRNS methodology, which is important for providing unbiased estimates of field-scale soil moisture to support applications in hydrology, remote sensing, and agriculture.

Plain Language Summary Measurements of root-zone soil moisture across spatial scales of tens to thousands of meters have been a challenge for many decades. The mobile application of Cosmic Ray Neutron Sensing (CRNS) is a promising approach to measure field soil moisture noninvasively by surveying large regions with a ground-based vehicle. Recently, concerns have been raised about a potentially biasing influence of roads. We employed physics simulations and dedicated experiments to quantify the influence of different road types on the CRNS measurement. We found that the presence of roads biased the CRNS estimation of field soil moisture compared to nonroad scenarios. Neutron measurements could overestimate the field value by up to 40 % depending on road material, width, surrounding field water content, and distance from the road. We proposed a correction function that successfully removed this bias and works even without prior knowledge of field soil moisture. Tests at different study sites demonstrated good agreement between corrected measurements and other field soil moisture observations. Our results constitute a practical advancement of the mobile CRNS methodology, which is important for providing unbiased estimates of field-scale soil moisture to support applications in hydrology, remote sensing, and agriculture.

1. Introduction

The monitoring of storage, movement, and quality of water at regional and global scales is of vital importance for practical applications such as agricultural production, water resources management, and predictions of hydrological extremes like floods and droughts (Seneviratne et al., 2010; Wood et al., 2011; Zink et al., 2016). To study land surface processes, soil moisture information is required at a scale relevant and representative of the physical, chemical, or biological processes of interest (Corwin et al., 2006; Entekhabi et al., 1999;

Gentine et al., 2012; Schulz et al., 2006; Vereecken et al., 2015). One of the grand challenges in soil moisture monitoring is the provision of parameters which describe these critical processes at the landscape scale and which represent the natural heterogeneity of the soil-hydrological system at scales of 1–1,000 m (Peters-Lidard et al., 2017; Robinson et al., 2008).

Over the last 10–15 years, satellite-based Earth observation technologies have made enormous progress toward mapping of soil moisture patterns at the catchment scale (Famiglietti et al., 2008; Kerr, 2007; Liu et al., 2011; Ochsner et al., 2013; Wagner et al., 2009; Wang & Qu, 2009). While such data are widely used today to calibrate large-scale hydrological models (Bates, 2012; Silvestro et al., 2015), its information content is often not appropriate to reveal processes at the intermediate scale up to 1,000 m (Western et al., 2002). The main shortcomings are the coarse spatial resolution, shallow measurement depth, and disturbing influences of vegetation and surface roughness (Robinson et al., 2008). In contrast to ground-based methods, atmospheric effects and geolocation introduce further uncertainty to remotely sensed products. When comparing the large spatiotemporal coverage of remote-sensing data against scales covered by local instruments (e.g., time-domain reflectometry, gravimetry, electromagnetic induction, gamma rays, and nuclear magnetic resonance; see Bogena et al., 2015), it becomes obvious that "there is currently a gap in our ability to routinely measure soil moisture at intermediate scales" (Robinson et al., 2008).

The method of Cosmic Ray Neutron Sensing (CRNS) for soil moisture estimation, introduced to the environmental science community by Zreda et al. (2008), provides a much larger measurement footprint than any other ground-based local method. With a support volume in the order of 10^4 m^3 ($>$100 m radius, $<$0.8 m depth; Köhli et al., 2015), CRNS has the potential to close the scale gap between point measurements of root-zone soil moisture and remotely sensed surface soil moisture (Montzka et al., 2017; Ochsner et al., 2013). The CRNS technology makes use of the extraordinarily high sensitivity of cosmic-ray neutrons to hydrogen nuclei and measures the concentration of epithermal neutrons above the soil surface. Since its introduction, the CRNS technology has quickly established itself in the field of hydrological observations (Andreasen et al., 2017) and is now used for soil moisture monitoring by many research groups worldwide (e.g., Bogena et al., 2013; Franz et al., 2013a; Peterson et al., 2016; Schrön et al., 2017; Zhu et al., 2016).

Pilot studies have shown the concept and potential of *mobile* CRNS (Desilets et al., 2010) using neutron detectors mounted on a ground-based vehicle ("rover"). The method is comparable to exploration missions with rovers on the Martian surface (Jun et al., 2013). Following advances on the understanding of stationary CRNS probes, recent studies have more and more elaborated on direct applications of the so-called *CRNS rover* (Avery et al., 2016; Chrisman & Zreda, 2013; Dong et al., 2014; Franz et al., 2015; McJannet et al., 2014, 2017). While the "classical," stationary CRNS application enables one to capture the hourly variability of soil moisture within a static footprint, the mobile application is intended to capture the spatial variability of soil moisture across larger areas or along large transects. The CRNS rover uses the same detection principle as the stationary CRNS probes but deploys multiple and larger neutron detectors in order to achieve higher count rates at much shorter recording periods.

Cultivated fields, forests, mountainous terrain, and private land are often not accessible by vehicles. Hence, the CRNS rover is usually moved along a network of existing roads, streets, and pathways in a study region. This strategy is also practical when the rover is used to cover large areas at the regional scale in a short period of time. However, recent neutron simulations by Köhli et al. (2015) showed that the stationary CRNS detector is particularly sensitive to the first few meters around the sensor. This was later confirmed by calibration and validation campaigns of stationary CRNS probes (Heidbüchel et al., 2016; Schattan et al., 2017; Schrön et al., 2017). This aspect is of high importance for the mobile application of CRNS. As a result of this local sensitivity, we hypothesize that the CRNS measurement is biased significantly when the moisture conditions present in the road differ substantially from the actual field of interest.

The effect of dry structures in the footprint was introduced for the first time by Franz et al. (2013a) and was also observed by Chrisman and Zreda (2013) and Schrön et al. (2018) on rover surveys through urban areas. Franz et al. (2015) sensed soil moisture of agricultural fields by roving on paved and gravel roads, and speculated that the road material could have introduced a dry bias to their measurements. It is critical to prove and quantify such an effect, not only for the advancement of the CRNS roving method, but also for its

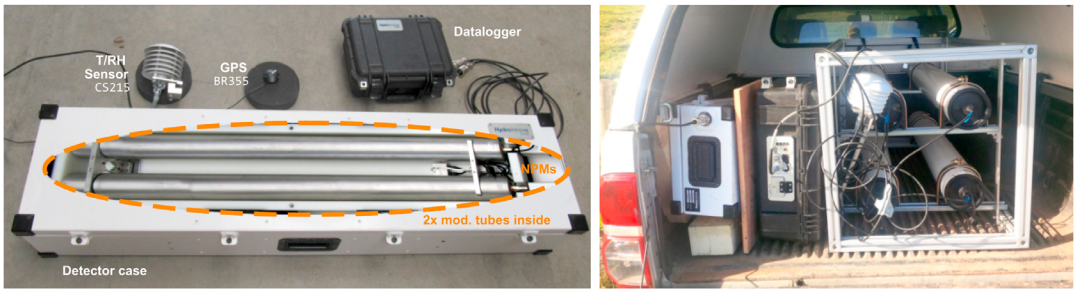

Figure 1. (left) Components of the CRNS rover system used in Germany, comprising two helium-3 gas tubes, external humidity and temperature sensors, a GPS unit, and the datalogger box including a battery. (right) A combination of detectors used in England, composed of the helium-3 system (white case), a small helium-3 unit (black case), and four boron trifluoride detectors (white tubes) which were disassembled from stationary probes.

application in agricultural irrigation management (Franz et al., 2015), for large-scale soil moisture retrieval to support hydrological modeling (Schrön, 2017; Zink et al., 2016), and for the evaluation of remote-sensing products (Montzka et al., 2017).

In the present study, we aim to evaluate and quantify the "road effect" by combining physical neutron transport modeling and dedicated field experiments. Based on theoretical investigations, we propose a universal correction function which is then tested and discussed in the light of ten rover campaigns in Central Germany and South England.

2. Methods

2.1. The Cosmic Ray Neutron Rover

The neutron background density in air is mainly controlled by the interaction of direct cosmic radiation with the ground and by the number of hydrogen atoms in the environment (Köhli et al., 2015; Zreda et al., 2008). As hydrogen is an elemental part of the water molecule, the correlation between the epithermal neutron signal and surrounding water storages can be beneficial for the monitoring of the hydrological cycle.

The cosmic ray neutron sensor makes use of thermal neutron detectors filled with helium-3 or boron trifluoride (Persons & Aloise, 2011; Schrön et al., 2018), manufactured by Hydroinnova LLC (Albuquerque, USA). A surrounding shield of polyethylene prevents most thermal neutrons in the natural radiation environment from entering the detector, while it slows down incoming, epithermal neutrons to detectable, thermal energies (Andreasen et al., 2016; Zreda et al., 2012; Köhli et al., 2018). Figure 1 shows a combination of the helium-3 detector system (white case, left), a small helium-3 unit (black case, middle), and four boron trifluoride tubes (right) which were disassembled from stationary probes.

The mobile CRNS detectors can be mounted in the trunk of a car. As neutrons are almost exclusively sensitive to hydrogen, the metallic material of the car appears almost transparent. Additional plastic components and human presence can result in a constant shielding factor, which is irrelevant for CRNS applications as only relative changes of neutrons are evaluated. Air temperature and humidity are recorded with sensors mounted externally to the car, because air conditions inside and outside can differ significantly. The neutron detector was set to integrate neutron counts over 1 minute. When in motion, this implicitly stretches the otherwise circular footprint to a patch elongated in the driving direction. In contrast, the GPS coordinates are read from a Globalsat BR-355 sensor at the time of recording, so after the neutron counts were integrated. To account for this artificial shift in postprocessing mode, the UTM coordinates of each signal were back-projected to half of the distance covered within that minute. Driving speed was adapted to local conditions and ranged from 15 to 80 m/min. The neutron count rate N depends on environmental moisture conditions and on the detector volume used. The helium-3 detector system observed 90–170 counts per minute (cpm) and showed a similar count rate as the sum of four boron trifluoride tubes. Three consecutive measurements (i.e., 3 min) underwent a moving-average filter to account for the moving footprint and to reduce the relative statistical uncertainty, $\sqrt{N}/N$, by a factor of $\sqrt{3}\approx 1.73$.

In order to obtain a proxy for near-surface water content, the detected neutron radiation needs to be corrected for the incoming variation of cosmic rays, for the air mass above the sensor, and for water vapor in the air (Schrön et al., 2015). In this work, we applied standard correction procedures (Hawdon et al., 2014; Rosolem et al., 2013; Zreda et al., 2012) in order to obtain a processed neutron count rate N.

To convert the neutron count rate to gravimetric soil water equivalent, θ_{grv}, several approaches have been proposed in literature. Desilets et al. (2010) suggested a theoretical relation that has been applied successfully by the majority of CRNS studies in the past. McJannet et al. (2014) found that this approach performs also better for rover campaigns than the universal calibration function proposed by Franz et al. (2013b), as the exact determination of soil and land use data is the major obstacle to apply the latter. The standard approach from Desilets et al. (2010) is as follows:

$$\theta_{grv}(N, N_0) = \frac{a_0}{N/N_0 - a_1} - a_2 \,, \tag{1}$$

where parameters $a_i = \{0.0808, 0.372, 0.115\}$ were determined using neutron physics simulations, and N_0 is a (site-specific) calibration parameter. The latter is determined once for each data set by comparing the CRNS soil moisture product with the actual soil moisture conditions in the field. However, neutrons are sensitive to all occurances of hydrogen in the footprint, such as ponds, organic material, lattice water, plant water, and other dynamic contributors. Hence, the variable $\theta_{grv}(N, N_0) = \theta_{sm} + \theta_{offset}$ denotes the sum of the soil water equivalent and an offset introduced by additional hydrogen pools. Furthermore, to compare CRNS products with other point sensors, the gravimetric water content is converted to volumetric water content, $\theta_{vol} = \theta_{grv} \cdot \varrho_{bd}$, using soil bulk density information ϱ_{bd}. In this work, we define

$$\theta(N) = \varrho_{bd} \left(\theta_{grv}(N, N_0) - \theta_{offset}\right) \tag{2}$$

as the CRNS soil moisture product, given in units of volumetric percent (%) throughout this manuscript.

To account for spatially variable parameters of soil bulk density and land use throughout the study area, additional sources of data were incorporated by recent studies (Avery et al., 2016; McJannet et al., 2017; Schrön, 2017). However, spatial information at the field scale (1–100 m) is often not available or comes with significant uncertainty. This can be considered a general handicap of the mobile CRNS method. In this work, we decided to apply the standard approach using spatially constant parameters, because (1) the selected study sites have sufficiently homogeneous soil and land use conditions and (2) the focus of the present study is to quantify the local effect of roads to the relative neutron signal, rather than the exact estimation of absolute soil moisture.

2.2. Simulation of Neutron Interactions With Road Structures

Theoretical calculations of the CRNS footprint by Köhli et al. (2015) have shown that the radial sensitivity of a CRNS detector is strongly influenced by the first few meters around the sensor (see also Schrön et al., 2017). Therefore, we hypothesized that nearby road material influences the neutron signal N, which differs from the signal N_{field} measured above the soil in the absence of a road. In this regard, we define the bias $N/N_{field} \neq 1$ describing the relative deviation of measured neutrons N on the road from measurements on the field, N_{field}, if the moisture contents of road and soil differ.

Many mobile surveys rely on road-only measurements of cosmic-ray neutrons. It can be expected that a potential road effect is larger when differences between road moisture and surrounding field water content are larger. It is highly impractical to measure the corresponding bias rigorously, as it might depend also on the road material (see above), on field soil moisture, and on the distance to the road. We therefore employed the Monte-Carlo technique using the neutron transport code URANOS (Köhli et al., 2015; www.ufz.de/uranos) to simulate the response of 10^2 to 10^4 eV neutrons to a domain of 25 ha which is crossed by a straight road geometry (see Figure 2).

The road is modeled as a 20 cm deep layer of either stone or asphalt, while the soil below was set to 5 % volumetric water content. Following the compendium of material composition data (McConn et al., 2011), asphalt pavement is modeled as a mixture of O, H, C, and Si, with an effective density of 2.58 g/cm^3, which corresponds to a soil water equivalent of $\theta_{road} \approx 12$ %. Stone/gravel is a mixture of Si, O, and Al, plus 3 % volumetric water content at a total density of 1.4 g/cm^3 (Köhli et al., 2015). The wetness of the surrounding soil, θ_{field}, has

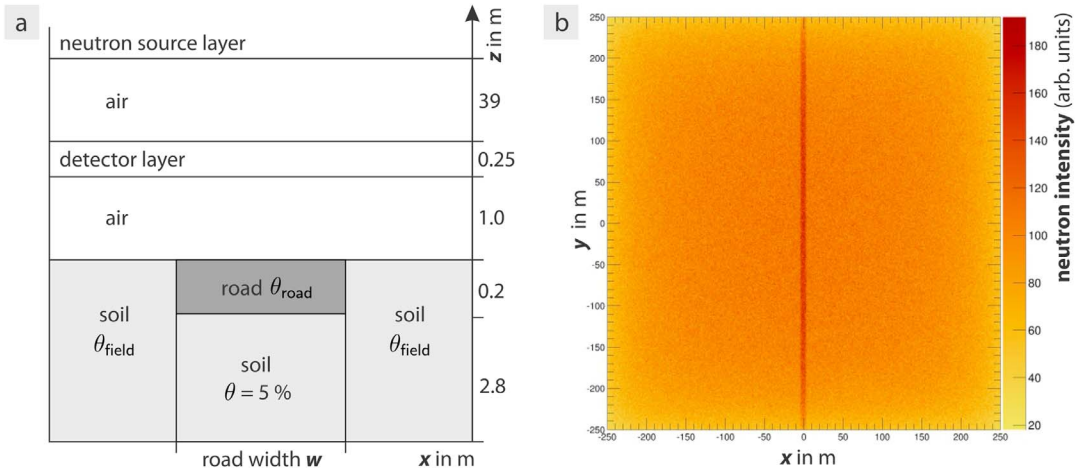

Figure 2. (a) Schematic of the model setup used by the Monte-Carlo code URANOS to simulate the response of cosmic ray neutrons to ground materials. (b) Exemplary URANOS model output showing a birds-eye view of the neutron density in the horizontal detector layer for a 5 m stoney road and 50 % field soil moisture.

been set homogeneously to 10, 20, 30, and 40 % volumetric water content. The neutron response to roads was simulated for road widths of 3, 5, and 7 m.

2.3. Validation With Point-Scale Measurements

Since the footprint of the CRNS signal covers an area of several hectares, comparison with point data is a challenge. To bridge this scale gap, Schrön et al. (2017) developed a procedure to calculate a weighted average of point samples, based on their distance and depth from the neutron detector. The method uses an advanced spatial sensitivity function based on neutron transport simulations by Köhli et al. (2015) and was successfully applied to calibration and validation data sets for stationary CRNS probes.

In our work presented here, we employed independent validation measurements of field moisture in the upper soil layer using occasional soil samples, and high frequency electromagnetic measurements with TDR100 (Campbell Scientific Ltd., Germany) and Theta Probes (Delta-T Devices, UK). Both instruments are standard approaches to determine soil permittivity which can then be converted to volumetric soil moisture (Roth et al., 1990). The Theta Probe measures soil system impedance at 100 MHz in the upper 6 cm, while the TDR100 evaluates pulse travel time in the GHz-range in the upper 10 cm (see also Blonquist et al., 2005; Vaz et al., 2013). The TDR100 has been redesigned for use in mobile field campaigns (Schröter et al., 2015). All instruments were individually calibrated using reference media with known dielectric properties (Kögler et al., 2013).

In order to compare the point measurements with the CRNS soil moisture product, a weighted average of the point data was applied based on their individual distance r to the neutron detector (see illustration circle in Figure 3). Using equations (1) and (2), the calibration parameter N_0 can be determined from the neutron count rate N and the independently measured value for average field soil moisture, $\langle\theta\rangle$. The soil moisture products were interpolated using an *Ordinary Kriging* approach, as the chosen measurement density adequately represents typical spatial correlation lengths of soil moisture at our study sites. The consistency between interpolated road and field data was assessed by probability density functions (PDFs) and scatterplots (see supporting information) of the soil moisture products. Since both data sets cover different spatial areas, only data from the overlapping areas (intersection) were included in the histogram analysis.

2.4. Experimental Setup

2.4.1. Road Types

Road moisture content is typically unknown and can only be determined by destructive sampling and lab analysis, or expensive geophysical exploration (Benedetto et al., 2012; Saarenketo & Scullion, 2000). In the scope of the uncertainties involved in roving neutron sensing, e.g., due to spatial heterogeneity of roads and surrounding land use, visual determination of the road material, guided by literature information, can

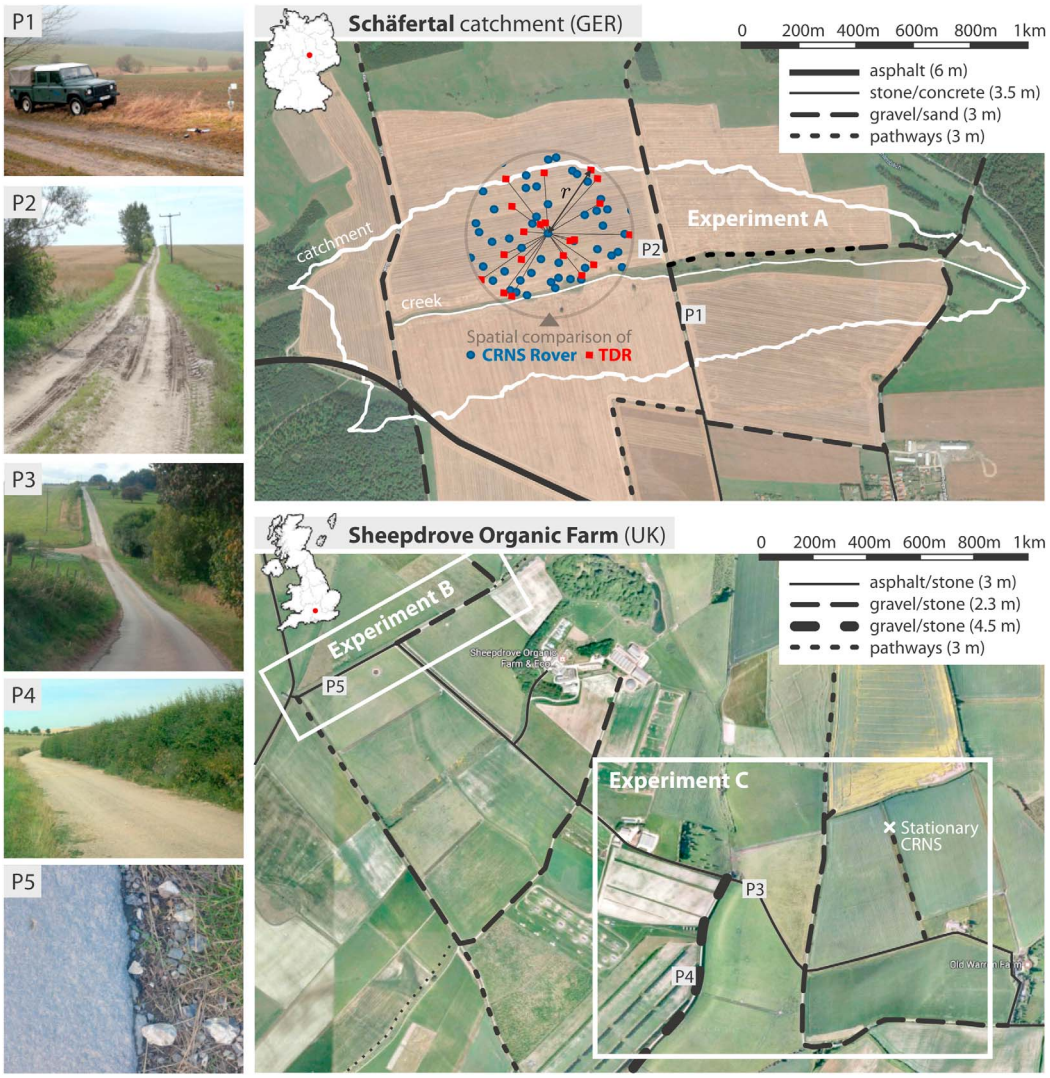

Figure 3. The study sites (top right) *Schäfertal* and (bottom right) *Sheepdrove Organic Farm*. White borders indicate the areas of three different field experiments A–C. Black lines indicate the type of road. The central circle with TDR points (red) and rover points (blue) illustrates the spatial calibration of the CRNS rover by comparing the large-scale neutron counts with point-scale soil moisture, using a weighted average of point samples based on their distance *r* to the rover. Pictures at certain spots: Schäfertal gravel/sand road (P1) and valley (P2), the Sheepdrove Farm valley (P3), Sheepdrove gravel/stone road (P4), and asphalt/stone road close-up (P5).

allow for an adequate estimate of its elemental composition and thus, its soil water equivalent. Chrisman and Zreda (2013) analyzed several samples of stone/concrete and asphalt in Arizona and found their *gravimetric* water equivalent to be 1.52 % and 5.10 %, respectively, including lattice water. Following literature values for typical material densities from 1.8 g/cm^3 (sandy concrete) to 2.4 g/cm^3 (hot asphalt; Houben, 1994; Stroup-Gardiner & Brown, 2000), the *volumetric* water equivalent then is ≈3 % and ≈12 %, respectively. As stone and asphalt are known as one of the most "dry" and "wet" road materials, respectively, we assumed the moisture content of the various road types in our study sites (Figure 3) to be within this range of extremes.

2.4.2. Schäfertal (Germany, Experiment A)

The *Schäfertal* site is a headwater catchment in the *Lower Harz Mountains* and one of the intensive monitoring sites in the *TERENO Harz/Central German Lowland Observatory* (51°39′N, 11°3′E; Wollschläger et al., 2016; Zacharias et al., 2011). The catchment covers an area of 1.66 km^2 and is predominantly under agricultural management. In the riparian zone at the valley bottom, grassland surrounds the creek *Schäferbach*. Grassland is also present at the outlet of the catchment and a forest occupies a small area at the north-eastern end

of the catchment outlet. Average bulk density of the soil is $\langle \varrho_{bd} \rangle = 1.55$ g/cm^3 and water equivalent of additional hydrogen and organic pools have been approximated to be $\langle \theta_{offset} \rangle = 2.3$ % in the mainly homogeneous bare field. Porosity and organic content are higher in the riparian zone. For more information about the local hydrology, see Martini et al. (2015) and Schröter et al. (2015).

Within the Schäfertal, Schröter et al. (2015, 2017) performed regular TDR campaigns by foot using 94 locations in the whole catchment area. During several campaigns from 2014 to 2016, the CRNS rover accompanied their team. Shortly after harvest the fields were accessible with the car, such that the same regions could be sampled with the rover and the TDR team on the same campaign day. On some days, however, the vehicle was not allowed to access the fields due to agricultural activities and seeded vegetation, such that CRNS measurements were taken only on the sandy roads which cross the agricultural fields and the creek.

The road network consists mainly of three types: a paved major road between the hilltops and the urban area, sandy roads within the catchment, and pathways along the creek. The paved road has an average width of 3.5 m and consists of a very dry stone/concrete mixture with an estimated 4 % volumetric water equivalent. The secondary roads are a mixture of stone, sand, and gravel, with 6 % moisture and 3 m width. The pathways are 3 m wide and contain mixed material from gravel, soil, and grass and have an estimated average moisture content of 10 %.

Rover measurements were taken using the helium-3 detector system at count rates of approximately 90–170 cpm, depending on wetness conditions. The corresponding neutron count uncertainties of 6–4 % propagated through equation (1) to absolute uncertainties in water equivalent, $\Delta\theta_{grv}$, of 10.0–0.9 gravimetric percent, for wet to dry conditions, respectively.

2.4.3. Sheepdrove Organic Farm (England, Experiments B and C)

The *Sheepdrove Organic Farm* is located on the *West Berkshire Downs* in the Lambourn catchment in South England (51°32′N, 1°29′W). The farm is located in a dry valley characterized by a highly permeable white chalk aquifer (Evans et al., 2016). Soil samples at the farm were collected at three fields with slightly different soil/vegetation characteristics between 2015 and 2017. The soil has a loamy clay texture with many flints and pieces of chalk, average bulk density is $\langle \varrho_{bd} \rangle = 1.25$ g/cm^3 and water equivalent of additional hydrogen and organic pools have been determined to be $\langle \theta_{offset} \rangle = 4.3$ % with insignificant differences between the fields.

The road network consists of a paved major road (width 3 m) made of an asphalt/stone mixture with an estimated moisture equivalent of 11 %. The main side roads are made of a gravel/stone mixture (7 %), most of which are 2.3 m wide, while the southern road is 4.5 m wide. Many nonsealed tracks (width 3 m) follow the borders between fields which partly consist of sand, grass, and organic material, such that their average moisture equivalent was estimated to 12 %.

Rover measurements were taken using the combination of the helium-3 detector system and the four boron trifluoride tubes at total count rates of approximately 180–330 cpm depending on wetness conditions. The corresponding neutron count uncertainties of 4–3 % propagated through equation (1) to absolute uncertainties in water equivalent $\Delta\theta_{grv}$ of 7.5–0.6 gravimetric percent, for wet to dry conditions, respectively.

3. Results and Discussions

3.1. Theoretical Investigations

Spatial Monte-Carlo simulations were performed to study the interactions of cosmic ray neutrons with roads of various widths, materials, and homogeneous field soil moisture conditions. The term "relative road bias" denotes the ratio of neutron intensity N detected in a road scenario (see Figure 2) over neutron intensity N_{field} detected in a scenario with a homogeneous soil moisture distribution.

Symbols in Figure 4 show the simulated road bias for a detector placed at the center of the road. The bias increases with increasing field soil moisture, increasing road width, and decreasing road moisture. The quantity is particularly sensitive to the water equivalent of the pavement (θ_{road}) and the soil (θ_{field}). Figure 5 plots the simulated road bias over distance from the road center, showing that the bias is a short-range effect that decreases a few meters away from the road, so that almost no measurable effect can be expected

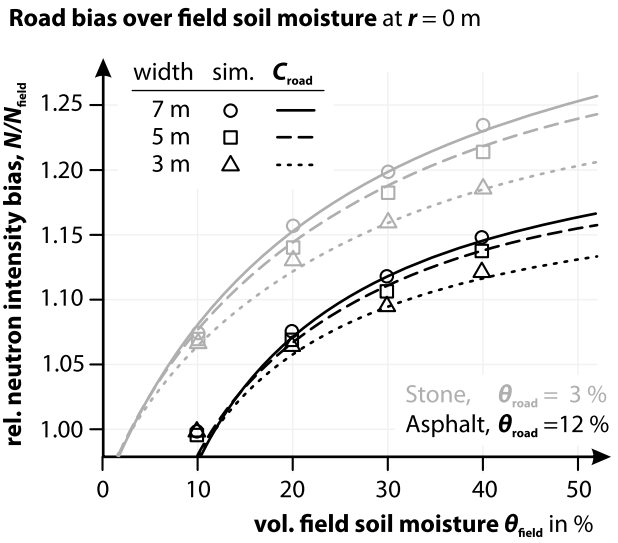

Figure 4. URANOS simulations (symbols) and fitted correction functions $C_{\mathrm{road}}(\theta_{\mathrm{field}}, \theta_{\mathrm{road}}, w, r)$ (lines) representing the neutron bias on roads of various widths through fields of different soil moisture. Shown for stone roads (grey) and asphalt roads (black). The quality of fit is in the range of ±0.01 except for rare cases with $\theta_{\mathrm{field}} < \theta_{\mathrm{road}}$.

beyond ≈10 m distance. It is evident from these simulations that the road bias is higher the larger the difference between road moisture and surrounding soil moisture, and the wider the road.

We suggest to correct the observed neutron intensity with a correction factor C_{road}, similar to the approaches used to correct for meteorological (Hawdon et al., 2014; Schrön et al., 2015) and biomass effects (Baatz et al., 2015):

$$N_{\mathrm{corr}} = N / C_{\mathrm{road}}\,, \tag{3}$$

where the correction factor should be 1 for no-road conditions, plus a product of terms that depend on the characteristics of the road and field conditions. The shape of each term of the proposed correction function is based on physical reasoning as follows:

1. The dependence on road width w is assumed to be a simple exponential, since the short-range dependency of neutron intensity on distance is exponential as shown by Köhli et al. (2015).
2. The dependence on water content (θ_{road} and θ_{field}) is assumed to be hyperbolic, since the natural response of neutrons to soil water exhibits a hyperbolic shape, as was derived from basic principles by Desilets et al. (2010) and Schrön (2017). This form (e.g., equation (1)) has been proven to be robust among all studies related to CRNS so far.
3. The dependence on distance r from the road center is assumed to be a sum of exponentials, since the combination of short-range and long-range neutrons indicate this relationship (see Köhli et al., 2015). An additional polynomial term ($w^a r^b$) might be necessary to account for the plateau introduced by the road of a certain width w.
4. Additionally, we demand that the total correction factor is 1 for road widths $w = 0$ as well as for similar moisture conditions in the road and in the field ($\theta_{\mathrm{road}} = \theta_{\mathrm{field}}$). The dependency on distance should be further normalized to 1 at the road center ($r = 0$).

The semianalytical approach was fitted to the URANOS simulation results. A minimum of 10 numerical parameters were required in order to adequately capture the most prominent features and dependencies of the simulated neutron response:

$$C_{\mathrm{road}}(\theta_{\mathrm{field}}, \theta_{\mathrm{road}}, w, r) = 1 + F_1(w) \cdot F_2(\theta_{\mathrm{field}}, \theta_{\mathrm{road}}) \cdot F_3(r, w)\,, \tag{4}$$

where

$$\begin{aligned} F_1(w) &= p_0\,(1 - e^{-p_1 w})\,, \\ F_2(\theta_{\mathrm{field}}, \theta_{\mathrm{road}}) &= (\theta_{\mathrm{field}} - \theta_{\mathrm{road}}) \frac{p_2 - p_3\,\theta_{\mathrm{road}}}{\theta_{\mathrm{field}} - p_4\,\theta_{\mathrm{road}} + p_5}\,, \\ F_3(r, w) &= p_6\, e^{-p_7 w^{-p_8} r^4} + (1 - p_6)\, e^{-p_9 r}\,. \end{aligned} \tag{5}$$

Table 1
Parameters p_i of the Parameter Functions F_j Describing the Road Correction Factor C_{road} (equation (5)), Namely the Geometry Term F_1, the Moisture Term F_2, the Distance Term F_3, and the Alternative Moisture Term F_2' That Does Not Require Prior Information About Field Soil Moisture (equation (6))

	p_0	p_1	p_2	p_3	p_4	p_5	p_6	p_7	p_8	p_9
F_1	0.42	0.50								
F_2			1.11	4.11	1.78	0.30				
F_3							0.94	1.10	2.70	0.01
F_2'			1.06	4.00	0.16	0.39				

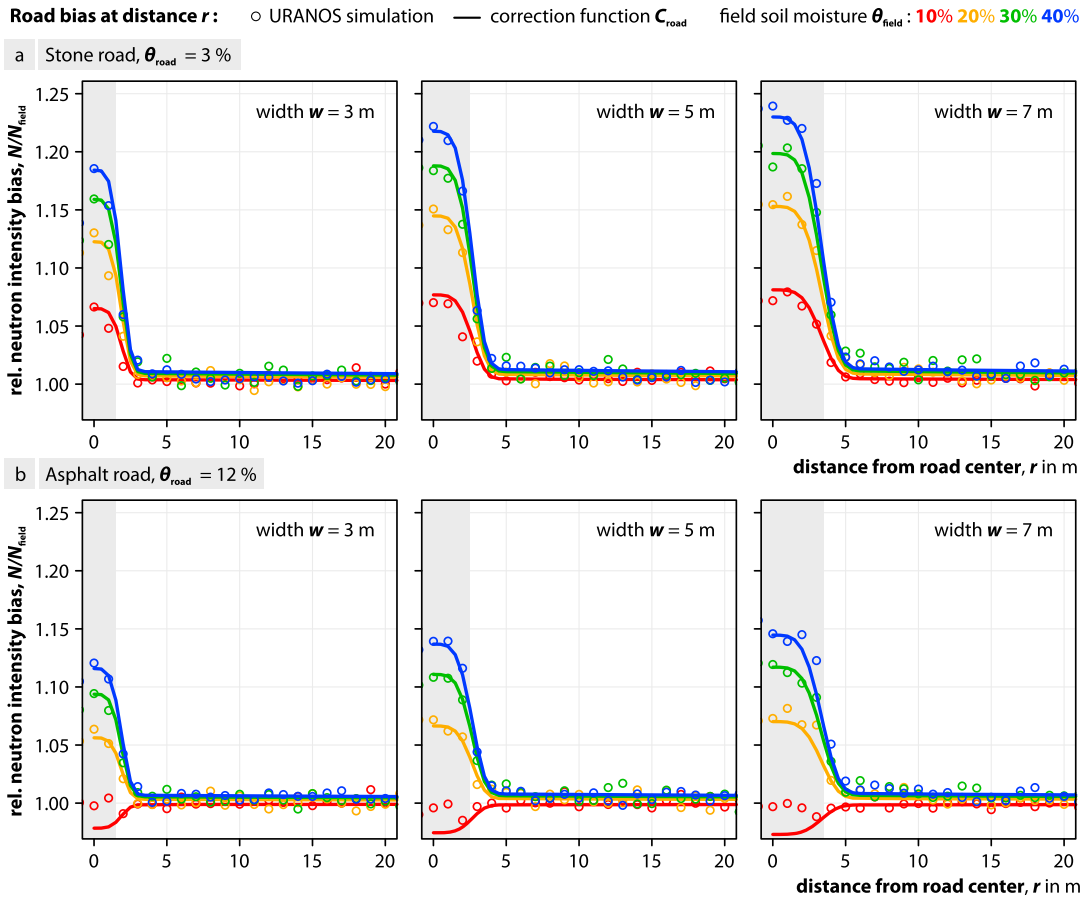

Figure 5. URANOS simulations (circles) and fitted correction functions $C_{\text{road}}(\theta_{\text{field}}, \theta_{\text{road}}, w, r)$ (lines) representing the neutron bias at different distances r from the road center ($r = 0$) for various road widths w (geometry shaded), field soil moisture (color), and (a) stone road material and (b) asphalt road material. Field conditions that are dryer than the road moisture (red in Figure 5b) cannot be represented by the analytical approach.

Parameters p_i of the geometry term F_1, the moisture term F_2, and the distance term F_3 are given in Table 1. Variables θ_{field} and θ_{road} are given in units of m^3/m^3, road width w and distance r are in units of m. The function is defined for road moisture values in the range of $1 \leq \theta_{\text{road}} \leq 16$ %.

The function fits well to the simulation results for different distances r from the road center (Figure 5), and for different θ_{field}, θ_{road}, and widths w (Figure 4). However, the performance of the analytical approach is poorer for road widths of 7 m and beyond (not shown). As the contribution of nonfield neutrons increases with road width, it is generelly not recommended to conduct surveys of field soil moisture on wide roads (compare also Schrön et al., 2017, Figure 11a). The approach also overestimates the absolute bias when the field soil moisture is lower than the road moisture. These rather unusual scenarios should be avoided when the function is applied to roving data sets in the future. Since simulation results have indicated that the influence of slightly wetter road material is insignificant, a redefinition of the form $F_2(\theta_{\text{road}} > \theta_{\text{field}}) = 1$ could be a sufficient approximation for these rare cases.

It is important to note that the moisture term F_2 depends on prior knowledge of the field soil moisture θ_{field}. The analysis of the field experiments in this work will investigate whether the moisture term can be replaced by a first-order approximation without prior knowledge.

3.2. Experiment A: Estimating Field Soil Moisture With TDR and the Rover

Our first field experiment was designed to test the capabilities of the cosmic ray neutron rover to capture small-scale patterns of soil moisture. During campaigns in the *Schäfertal*, the rover was moved across the

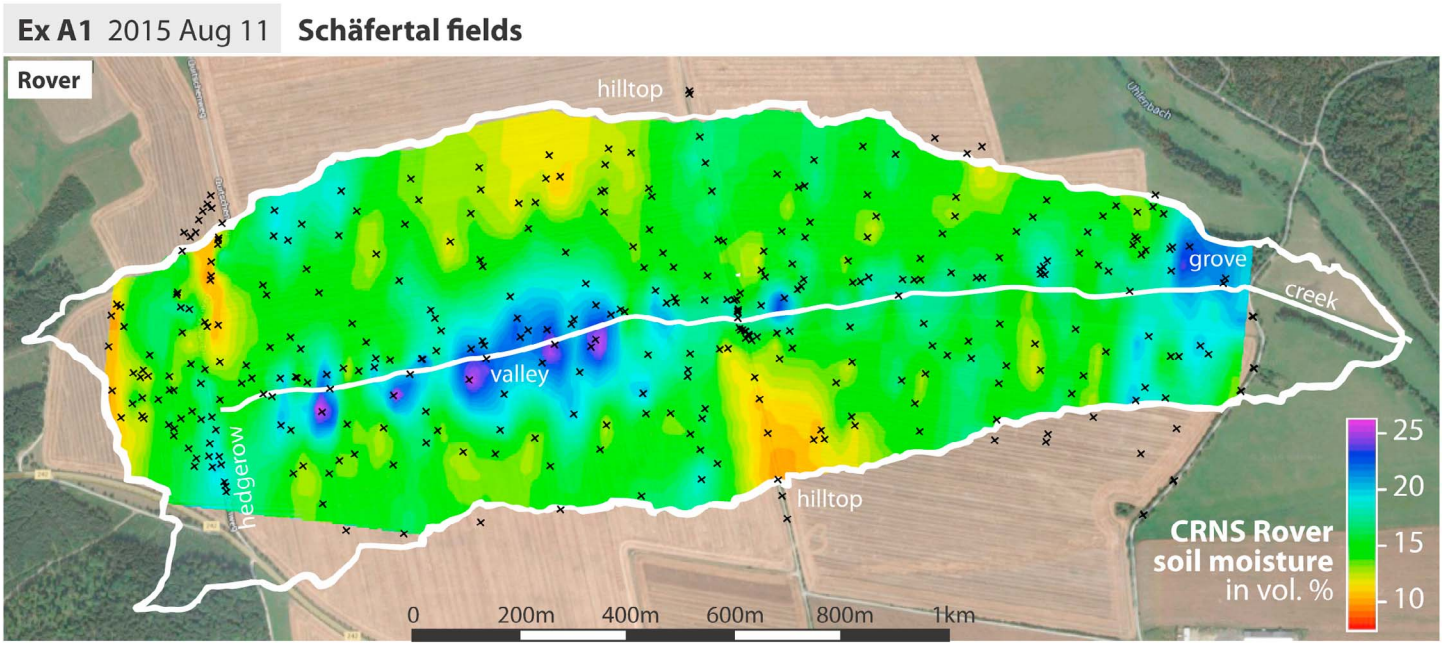

Figure 6. Soil moisture estimation by the CRNS rover in the *Schäfertal* agricultural field. Data were interpolated from points (black cross) which represent the central location of the path travelled by the rover within the one minute acquisition time. Actual hydrological features like contact springs in the valley and dry hilltops are evident, but other influences of the grove, the hedgerow, and roads (see also Figure 3) may distort the derived soil moisture values, indicating challenges of the method.

fields over the course of 4–6 h. At the rate of one data point per minute, the technology allowed collection of more than 200–400 data points in the catchment, which is an adequate number to justify ordinary kriging within the 1.66 km^2 area.

Figure 6 shows the highly resolved CRNS soil moisture product which reveals hydrological features in the catchment, such as dry hilltops, or contact springs in the valley near the creek due to shallow groundwater. Since the data were not corrected for biomass water, a probable influence of vegetation can be seen near the grove in the north-eastern part of the catchment, and possibly also near the hedgerow (south-western part). While the experiment focused on the agricultural areas of the harvested field and thus surveyed across the field and along its borders, a few roads were touched briefly at the southern and north-western hilltops, where the soil appears to be slightly drier.

Figure 7 summarizes results from this and other field surveys in the *Schäfertal* that were conducted together with a team using handheld TDR devices. Using 94 TDR samples and more than 300 rover points in experiment A1, it was possible to find a calibration factor N_0=10,447 cph (equation (1)) that explained all six subexperiments in the catchment area. In August 2015 (Figures 7a and 7b), all the fields of the *Schäfertal* site were accessible with the car, however, TDR campaigns were incomplete due to technical issues. In the summer of 2014 (Figures 7c and 7d), only the northern fields could be surveyed due to agricultural activities in the southern area. For all of the first four campaign days, Figures 7a–7d, a good agreement between the rover and the TDR products in representing patterns and mean soil moisture in the *Schäfertal* was achieved. Besides the visual impression in columns 1 and 2, the probability density functions (PDFs) of their overlapping area (third column) confirm emphatically that the main soil moisture patterns were well captured by both methods. An additional perspective on the data is provided by scatterplots in the supporting information.

The two approaches appear to show remarkable agreement, despite the fact the two data sets were technically different. First, the penetration depths of both methods were different, TDR measured in the upper 10 cm of the soil, while CRNS integrated down to 20–50 cm, though with highest sensitivity to the upper 10 cm (Schrön et al., 2017). Second, TDR data was too sparse to achieve a comparable interpolation quality, especially on days when less than a few tens of data points were available (Webster & Oliver, 1992). Third, spatially constant parameters, N_0, ϱ_{bd}, θ_{offset}, were used for the conversion from neutrons to soil moisture (equations (1) and (2)). In strong contrast, rover measurements at the last two survey days, Figures 7e and 7f, show a poor

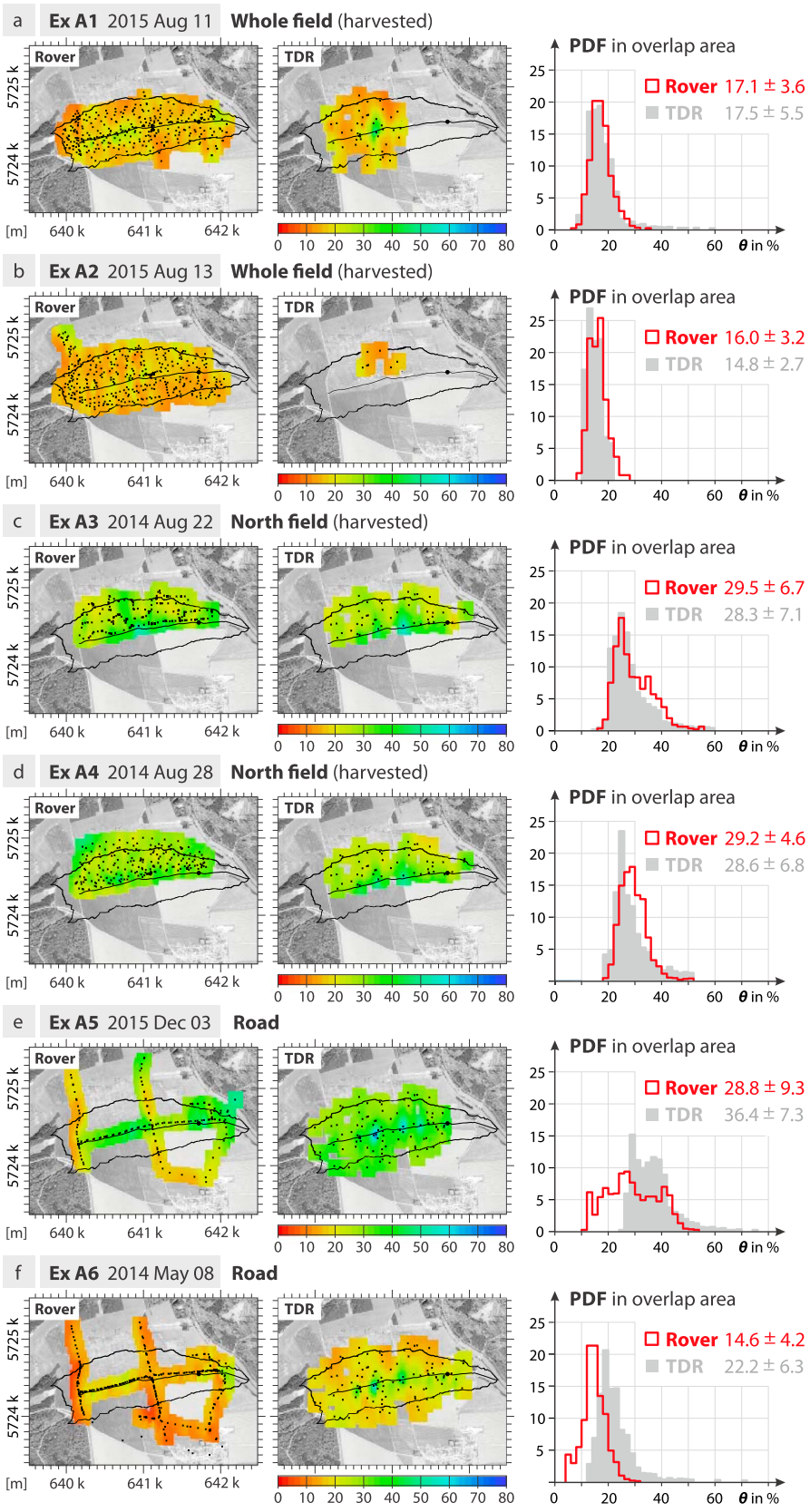

Figure 7. Comparison of CRNS Rover and TDR campaigns in the *Schäfertal* using interpolated data, and the probability density functions (PDF) of soil moisture in their overlapping area. See also the corresponding scatterplots in the supporting information.

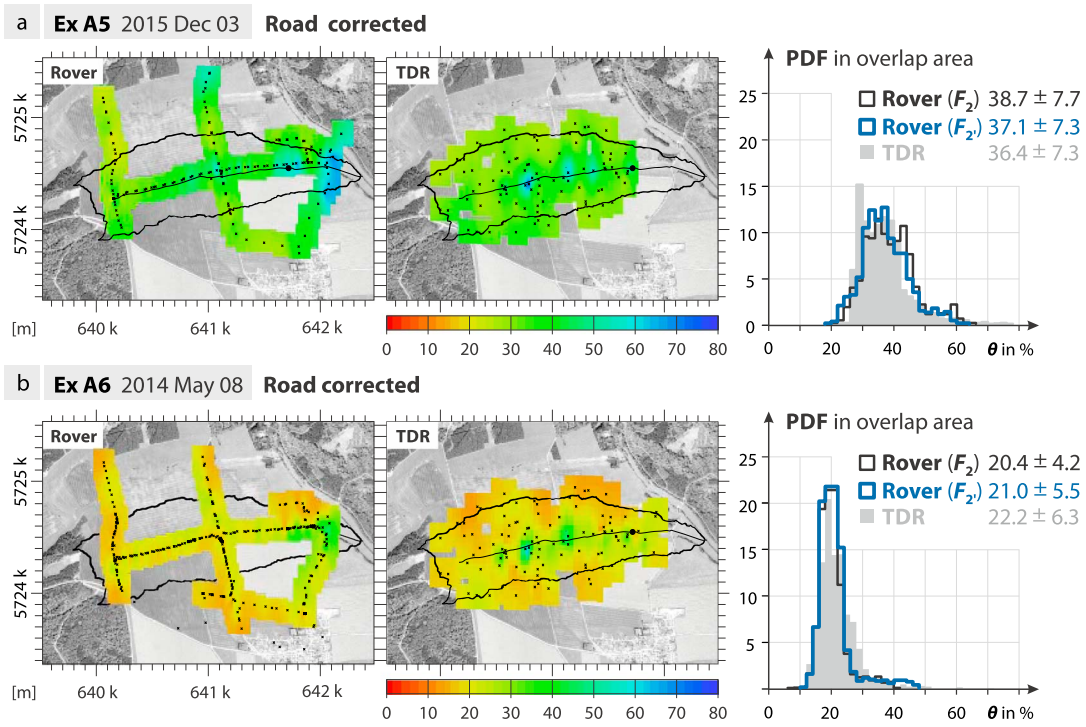

Figure 8. Application of the road correction approach on the road-only surveys in the *Schäfertal* (compare Figures 7e and 7f). Patterns of (left) the rover agree well with those from (middle) TDR in terms of (right) the probability density function in the overlap area of both interpolated grids, their mean, and standard deviation. The correction is tested with two approaches of the moisture term: (1) $F_2(\theta_{\text{field}}=\langle\theta_{\text{TDR}}\rangle)$ (equation (5)) using the average of the TDR data (black line) and (2) $F_{2'}(\theta(N))$ (equation (6)) using uncorrected neutron counts as a proxy (blue line). Kriging results using the former approach were almost identical to those using the latter approach, so that only the latter is shown in the left plot. Corresponding scatterplots are presented in the supporting information.

agreement to field soil moisture measured by TDR. At those days, the CRNS rover had no access to the field and only crossed nearby roads and pathways. The corresponding impact on data interpretation is discussed in section 3.3.

The field campaigns highlight characteristic hydrological features, e.g., the mentioned contact springs near the creek, that are especially prominent during dry periods and were identified also by other researchers using conventional measurement techniques (Graeff et al., 2009; Schröter et al., 2015). The experiment shows that the rover can efficiently contribute to hydrological process understanding, while the assumption of spatially constant parameters is considered acceptable for the relatively homogeneous *Schäfertal* site.

3.3. Taking the Road Effect Into Account

In May 2014 and December 2015, the fields were cultivated and the CRNS rover surveys were restricted to the roads. Those campaigns are shown in Figures 7e and 7f, where the effect of the dry road is clearly visible in all plots. This result indicates that measurements from the road are biased and therefore not representative for field soil moisture. Under wet conditions, the probability density function (PDF) of soil moisture does not reflect the field conditions (Figure 7e), while under dry conditions there seems to be a simple bias of the histogram toward the dry end (Figure 7f).

The presented road-effect correction approach promises to account for this behavior, as it scales with the difference between road and field moisture, using information of the different types of roads crossing the catchment (Figure 3). The correction function C_{road} was applied using prior knowledge about the mean field soil moisture (equation (5)). The use of $\theta_{\text{field}}=\langle\theta_{\text{TDR}}\rangle$ led to better agreement between the rover and the TDR data for both days as shown in Figure 8 (black histograms).

However, in most cases independent measurements of field soil moisture θ_{field} are not available. As an alternative, the first-order approximation of soil moisture, $\theta(N)$, using the uncorrected neutron count rate N,

could be used as a proxy to estimate the bias due to the difference in soil moisture between road and field. An alternative analytical approach for the moisture term F_2 (equation (5)) is proposed here that essentially accounts for the mismatch between $\theta(N)$ and θ_{field}:

$$F_{2'}(\theta(N), \theta_{\text{road}}) \approx p_2 - p_3\,\theta_{\text{road}} - \frac{p_4 + \theta_{\text{road}}}{p_5 + \theta(N)}\,. \tag{6}$$

The updated empirical parameters p_{2-5} (Table 1) were determined based on the data sets of the *Schäfertal* and another, independent experiment in the context of an interdisciplinary research project which included rover measurements across different land use types (Scale X, see also Wolf et al. (2016), data not shown here). Although the approach is empirical, the preliminary tests at four different sites in the UK and Germany indicate that the method might be transferable. The corresponding probability distribution is indicated by the blue line in Figure 8, showing that the two approaches led to almost identical results.

3.4. Experiment B: Road Influence at a Distance

The experiments at the *Sheepdrove Farm* aimed to compare the soil moisture patterns of the road and the field, by surveying both compartments with the rover and excluding one of them during the analysis. The general objective of these experiments was to clarify whether the road correction function can be used to transfer the apparent soil moisture patterns seen from the road to values that were taken in the actual field.

The road network across the farm is an ideal location to test the road-effect correction, due to its wide range of road materials (gravel to asphalt) and road widths (2.3–4.5 m). To improve the accuracy of the rover measurements, the count rate was increased by combining multiple neutron detectors. Each of the rover data sets (experiments B and C) were compared to a stationary, well-calibrated CRNS probe and to occasional Theta Probe measurements (not shown), in order to find a universal calibration parameter N_0=11,300 cph (see also equation (1)) for all data sets.

In order to rigorously test the theoretically predicted dependency of the road bias on the road moisture θ_{road} and the distance r to the road center, a dedicated experiment was performed at the north-west corner of the *Sheepdrove Farm* (Figure 9a). A gravel/stone road (north) and an asphalt/stone road (south) are aligned almost linearly and meet centrally at a junction. The road moisture reflects the mixture of present road materials and was estimated to be ≈11 for the asphalt/stone mix, and ≈7 % for the gravel/stone mix.

The rover measured neutrons along parallel lines in various distances from the road. For each track, the corresponding mean and standard deviation were calculated, which represent mainly the heterogeneity of soil and vegetation along each of the 400 m tracks. Figure 9b shows how the influence of the road decreases the apparent field soil moisture as measured by the rover (left). Upon application of the road correction function, measurements converge to similar values for all distances (right) and reveal different soil moisture conditions for the nothern and southern fields. The apparent increase at $r = 12$ m is likely caused by hydrogen present in the hedgerow and the nearby grove. The overall result provides evidence that the analytical correction function properly represents the road bias at different distances and for different materials.

3.5. Experiment C: Patterns Across Roads and Fields

On three different campaign days, the roads and the surrounding fields in the central valley of the *Sheepdrove Farm* were surveyed with the CRNS rover. Road points were corrected using equations (4) and (6) based on the road types shown in Figure 3. The corresponding soil moisture maps and histograms (PDFs) are shown in Figure 10, where the three campaign days are denoted as C1–C3.

In experiment C1, it was only possible to access the borders of the field (r=10±5 m) due to farming activities. Nevertheless, the correction of the road data set led to adequate improvement of the average soil moisture distribution (Figure 10). However, some patterns were not adequately resolved by the road survey. According to the field measurements, the central northern field was wetter than the central southern field. From measurements on the road, only an average water content was seen with no distinction between the two fields. There were also discrepancies in the eastern part of the farm, where road and field patterns seemed to be inverse. It can be speculated that one reason for this behavior is the influence of the south-eastern field, which was not surveyed on that day. The dry spot at the north-west corner is due to buildings and a large concrete area, which were not accounted for in the correction procedure.

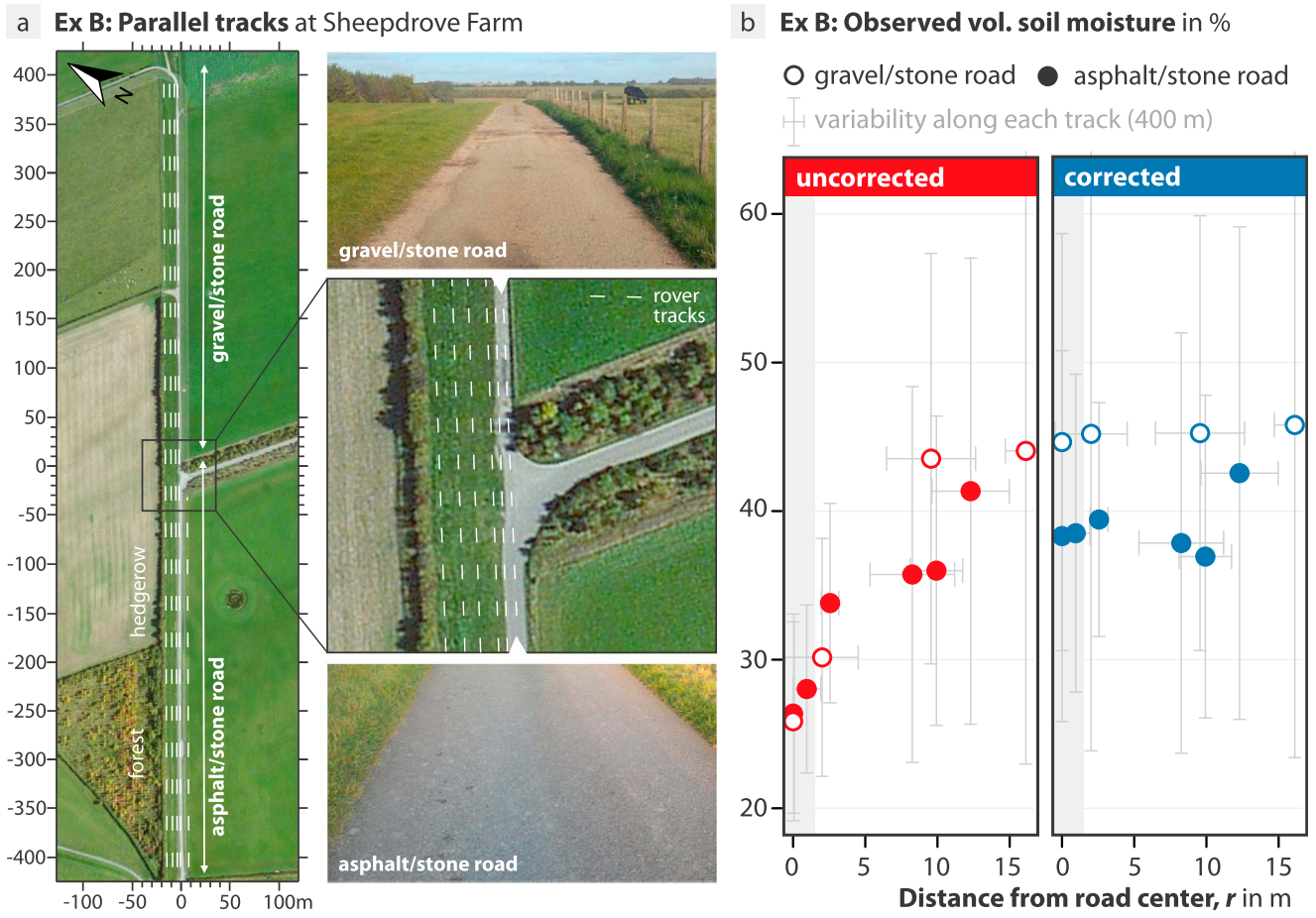

Figure 9. Experiment B at the *Sheepdrove Farm*. (a) Parallel tracks (dashed) at different distances from two roads of different materials that meet at the junction ($x = 0$, $y = 0$). (b) (left) The influence of the road decreases the apparent field soil moisture measured by the rover. (right) After application of the road correction function, measurements converge to similar values for all distances and reveal different soil moisture conditions for the nothern and southern fields. Error bars indicate the heterogeneity of water content along the 400 m track length.

In experiment C2, it was possible to fully cross the fields to generate an adequate interpolation of field soil moisture. The correction of all road types appeared to agree very well with the overall pattern of the field measurements (Figure 10). The probability density functions show good agreement in the overlapping area of both data sets (i.e., near the road).

The road correction in experiment C3 was also able to capture the patterns seen by the field survey, with the exception of the wet region in the northern part. It is speculative whether oversaturated road material, temporary ponds on the road, or local vegetation influenced the data collected by the rover. This pathway is lowered by 1–2 m compared to the field, however, the potential influence of the local terrain features on the CRNS performance was not quantified in the scope of this study. Additional vegetation correction could probably reduce the apparent soil moisture in this part, which is surrounded by unmanaged grass and hedges. In any case, low precipitation (drizzle) might have added interception water during this day, which is almost impossible to quantify.

All in all, the consistency between road and field measurements was improved by the application of the road correction approach in terms of mean, standard deviation, and root-mean-square error (see also supporting information). Some of the patterns in the field were invisible from the road, especially when significant differences in soil moisture were present between neighboring fields passed by the rover. In these cases, it is not possible for the sensor to capture the corresponding patterns due to the isotropic nature of neutron detection. Moreover, local ponds on pathways or nearby unmanaged vegetation could further influence the neutron signal in a way that is not representative for the field. These structures often contain or intercept water that can act as a shield for neutrons from the field behind.

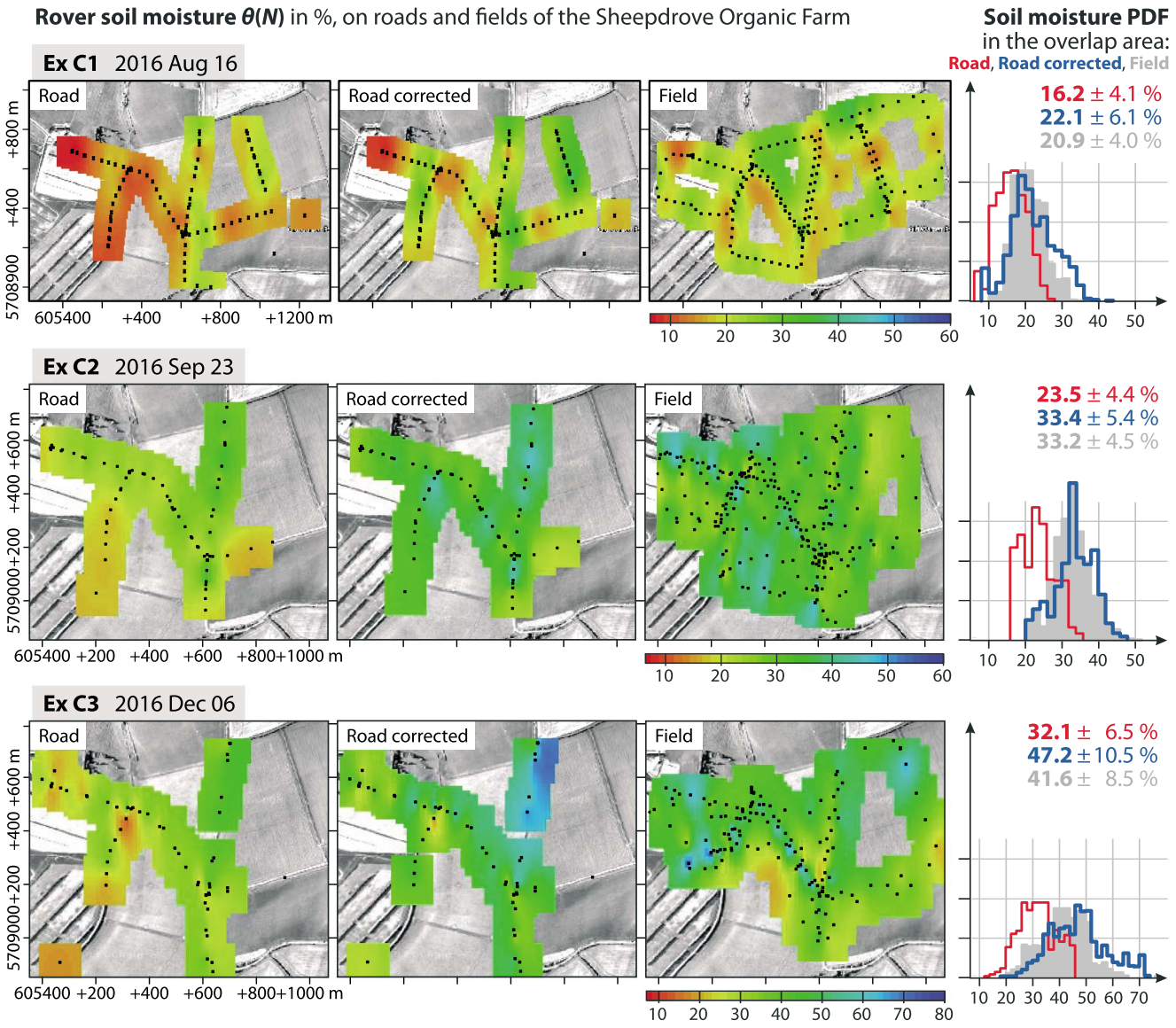

Figure 10. Interpolated soil moisture inferred from rover measurements for experiments C1–C3, showing (left) uncorrected road data, (middle) corrected road data, and (right) field data. Next to it, the probability density functions of data in the overlapping areas show that the corrected road data (blue) can represent the field data (grey) better than the uncorrected road data (red). Mean and standard deviation of each distribution are provided in the top right corner. Performance in terms of root-mean-square errors (RMSE) is given in the supporting information.

3.6. Tradeoff Between Measurements From the Road and the Field

Although it is evident that neutron measurements on the road can be biased substantially, it remains a challenge for experimentalists to access nonroad areas, because either the access of fields is restricted or campaigns are required to cover large areas in a reasonable amount of time. Hence, roving on roads is much more practical and a necessary condition to travel from site to site. The campaigns in the *Sheepdrove Farm* combine both, road and field data, from which it could be inferred which number of measurements in the field is needed, in addition to the road data, to obtain an acceptable estimate of the field soil moisture.

In Figure 11, all data points obtained during each campaign were bootstrapped, leading to more than 2,000 combinations of road and field measurements. The figure shows that the inclusion of uncorrected road points (red) can lead to an unreliable average value. Depending on wetness conditions, at least 80–95 % of the data points should be taken in the field to obtain an average that is within a 2 % accuracy range

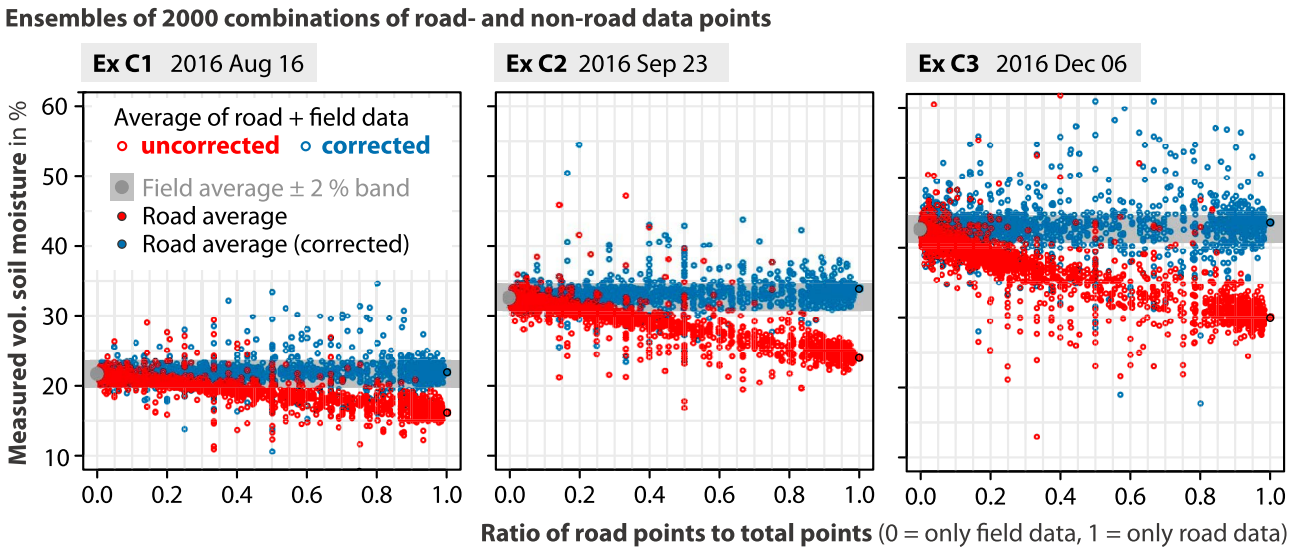

Figure 11. Apparent average soil moisture for 2,000 combinations of road and nonroad (i.e., field) points in experiments C1–C3 plotted as a function of the fraction of selected road points in the ensemble to the total number of selected points (i.e., sum of road and field). Data are shown for uncorrected (red) and corrected (blue) road effects. If data are not corrected, a maximum fraction of road points between 0.20 and 0.05 is acceptable (under dry or wet conditions, respectively) to obtain a realistic estimate of field soil moisture within 2 % accuracy.

around the mean field water content. In contrast to uncorrected data, corrected road data (blue) are already good predictors for field soil moisture when any number of survey points on the road and in the field are averaged.

The analysis shows that any combination of field data and corrected road data can lead to a sufficiently accurate estimation of average water content in the survey area. However, the correction procedure is highly sensitive to supporting information like road moisture, field moisture, and road width (see Figure 4). If these parameters are uncertain, their impact on the CRNS product could be substantial. The impact could be reduced by calibrating the road correction parameters with road and field data at selected anchor locations, or by including a substantial number of field data points in the data set measured only on roads.

4. Conclusions

The mobile cosmic ray neutron sensor (CRNS rover) was successfully applied to estimate soil moisture at scales from a few meters to a few square kilometers. One of the most prominent insights from the detailed and extensive investigations is the confirmation that the CRNS rover is capable of capturing small-scale patterns at resolutions of 10–100 m. This result opens the path for noninvasive tomography of root-zone soil moisture patterns in small catchments and agricultural fields, where traditional methods would require exhaustive and time-consuming efforts.

The study revealed the critical need to apply correction approaches to account for the local effects of dry roads. The different experiments carried out in the course of this study showed a critical loss in the capability to estimate average field soil moisture when the field was not accessible and the measurements were taken on roads only. This effect was quantified in this study for the first time using neutron transport simulations, and confirmed by dedicated experiments.

We propose an analytical correction function which accounts for road type and soil moisture conditions. As the analytical form of the corresponding relations was based on physical reasoning, and the parameters were determined with the help of neutron simulations, the approach can be assumed to be universally applicable. However, the analytical fit showed a few limitations for roads that are wetter than the field, and for roads wider than 7 m. The approach is further sensitive to the road parameters like width w and moisture θ_{road}. While the measurement of road moisture content is impractical, this quantity could be treated as a calibration parameter by comparing data on the road and in the field at certain anchor locations.

The correction approach further depends on prior knowledge of field soil moisture (equations (4) and (5)). To circumvent this requirement, an adaption of the equation has been proposed that takes the uncorrected first-order approximation, $\theta(N)$, as a proxy instead (equation (6)). Although we have shown its performance for the two, climatologically similar sites on ten different days throughout the years, the empirical character of this alternative approach (see section 3.3) requires more tests at more sites and different conditions.

The corrected road data were compared with field soil moisture inferred from independent TDR (experiment A) and rover measurements (experiments B and C). In all cases the corrected soil moisture product sensed from the road was more consistent with the overall pattern, the mean, and the standard deviation of soil moisture in the field. However, the method has problems to resolve patterns when fields on the left and right from the road have different soil water contents or are located behind hedges.

Nevertheless, a considerable amount of uncertainty is introduced to measurements from roads due to the high contribution of nonfield neutrons and the uncertain properties of the road and its surroundings. Therefore, it is advisable to avoid wide roads, to drive directly on the field wherever possible, or to take additional measurements on the field every now and then. This is advisable not only to make sure that the parameters of the road correction lead to a proper representation of field soil moisture, but also to support spatial interpolation. In future campaigns, capturing imagery could be a potential advancement to support the estimation of material parameters for roads and vegetation along the track.

Based on the conclusions above, we generally recommend to correct for the road effect before spatial CRNS data are used to support hydrological models or agricultural decisions. With regards to evaluation of remote-sensing products (e.g., Chrisman & Zreda, 2013) dry roads are also part of the remotely sensed average soil moisture, so that different correction approaches might be needed to compare both area-averaged products. There might also be ways to reduce the contribution of the roads in future developments of the neutron detector. For example by mounting the detector on top of the car where it is more exposed to far-field neutrons.

Acknowledgments
Data of the CRNS rover measurements are included as supporting information. M.S., R.R., and J.I. thank Dan Bull for providing access to the Sheepdrove Organic Farm. M.S., I.S., and U.W. thank Thomas Grau, Mandy Kasner, and Andreas Schmidt for their support during field campaigns in the Schäfertal. M.S. acknowledges kind support by the Helmholtz Impulse and Networking Fund through Helmholtz Interdisciplinary School for Environmental Research (HIGRADE). J.I. is funded by the Queen's School of Engineering, University of Bristol, EPSRC, grant EP/L504919/1. R.R., J.I., and Sheepdrove Organic Farm activities are funded by the Natural Environment Research Council (A MUlti-scale Soil moisture Evapotranspiration Dynamics study [AMUSED]; grant NE/M003086/1). We acknowledge the NMDB database (www.nmdb.eu), founded under the European Union's FP7 programme (contract no. 213007) for providing data for incoming radiation, especially from monitors Jungfraujoch (Physikalisches Institut, University of Bern) and Kiel (Institute for Experimental and Applied Physics, University of Kiel). The research was funded and supported by the Terrestrial Environmental Observatories (TERENO), which is a joint collaboration program involving several Helmholtz Research Centers in Germany.

References

Andreasen, M., Jensen, H. K., Zreda, M., Desilets, D., Bogena, H., & Looms, C. M. (2016). Modeling cosmic ray neutron field measurements. *Water Resources Research*, *52*, 6451–6471. https://doi.org/10.1002/2015WR018236

Andreasen, M., Jensen, K. H., Desilets, D., Franz, T. E., Zreda, M., Bogena, H. R., et al. (2017). Status and perspectives on the cosmic-ray neutron method for soil moisture estimation and other environmental science applications. *Vadose Zone Journal*, *16*(8).

Avery, W. A., Finkenbiner, C., Franz, T. E., Wang, T., Nguy-Robertson, A. L., Suyker, A., et al. (2016). Incorporation of globally available datasets into the roving cosmic-ray neutron probe method for estimating field-scale soil water content. *Hydrology and Earth System Sciences*, *20*, 3859–3872. https://doi.org/10.5194/hess-20-3859-2016

Baatz, R., Bogena, H. R., Franssen, H.-J. H., Huisman, J. A., Montzka, C., & Vereecken, H. (2015). An empirical vegetation correction for soil water content quantification using cosmic ray probes. *Water Resources Research*, *51*, 2030–2046. https://doi.org/10.1002/2014WR016443

Bates, P. D. (2012). Integrating remote sensing data with flood inundation models: How far have we got? *Hydrological Processes*, *26*(16), 2515–2521.

Benedetto, A., Benedetto, F., & Tosti, F. (2012). Gpr applications for geotechnical stability of transportation infrastructures. *Nondestructive Testing and Evaluation*, *27*(3), 253–262. https://doi.org/10.1080/10589759.2012.694884

Blonquist, J., Jones, S. B., & Robinson, D. (2005). Standardizing characterization of electromagnetic water content sensors. *Vadose Zone Journal*, *4*(4), 1059–1069.

Bogena, H. R., Huisman, J. A., Baatz, R., Hendricks Franssen, H.-J., & Vereecken, H. (2013). Accuracy of the cosmic-ray soil water content probe in humid forest ecosystems: The worst case scenario. *Water Resources Research*, *49*, 5778–5791. https://doi.org/10.1002/wrcr.20463

Bogena, H. R., Huisman, J. A., Güntner, A., Hübner, C., Kusche, J., Jonard, F., et al. (2015). Emerging methods for noninvasive sensing of soil moisture dynamics from field to catchment scale: A review. *Wiley Interdisciplinary Reviews: Water*, *2*(6), 635–647.

Chrisman, B., & Zreda, M. (2013). Quantifying mesoscale soil moisture with the cosmic-ray rover. *Hydrology and Earth System Sciences*, *17*(12), 5097–5108. https://doi.org/10.5194/hess-17-5097-2013

Corwin, D. L., Hopmans, J., & de Rooij, G. H. (2006). From field-to landscape-scale vadose zone processes: Scale issues, modeling, and monitoring. *Vadose Zone Journal*, *5*(1), 129–139.

Desilets, D., Zreda, M., & Ferré, T. (2010). Nature's neutron probe: Land surface hydrology at an elusive scale with cosmic rays. *Water Resources Research*, *46*, W11505. https://doi.org/10.1029/2009WR008726

Dong, J., Ochsner, T. E., Zreda, M., Cosh, M. H., & Zou, C. B. (2014). Calibration and validation of the cosmos rover for surface soil moisture measurement. *Vadose Zone Journal*, *13*(4). https://doi.org/10.2136/vzj2013.08.0148

Entekhabi, D., G. R., Asrar, A. K., Betts, K. J., Beven, R. L., Bras, C. J., Duffy, T., et al. (1999). An agenda for land surface hydrology research and a call for the second international hydrological decade. *Bulletin of the American Meteorological Society*, *80*(10), 2043–2058.

Evans, J., H., Ward, J., Blake, E., Hewitt, R., Morrison, M., Fry, L., et al. (2016). Soil water content in southern england derived from a cosmic-ray soil moisture observing system—COSMOS-UK. *Hydrological Processes*, *30*(26), 4987–4999.

Famiglietti, J. S., Ryu, D., Berg, A. A., Rodell, M., & Jackson, T. J. (2008). Field observations of soil moisture variability across scales. *Water Resources Research*, *44*,W01423. https://doi.org/10.1029/2006WR005804

Franz, T., Wang, T., Avery, W., Finkenbiner, C., & Brocca, L. (2015). Combined analysis of soil moisture measurements from roving and fixed cosmic ray neutron probes for multiscale real-time monitoring. *Geophysical Research Letters*, *42*, 3389–3396. https://doi.org/10.1002/2015GL063963

Franz, T. E., Zreda, M., Ferré, T. P. A., & Rosolem, R. (2013a). An assessment of the effect of horizontal soil moisture heterogeneity on the area-average measurement of cosmic-ray neutrons. *Water Resources Research*, *49*, 6450–6458. https://doi.org/10.1002/wrcr.20530

Franz, T. E., Zreda, M., Rosolem, R., & Ferré, T. P. A. (2013b). A universal calibration function for determination of soil moisture with cosmic-ray neutrons. *Hydrology and Earth System Sciences*, *17*(2), 453–460. https://doi.org/10.5194/hess-17-453-2013

Gentine, P., Troy, T. J., Lintner, B. R., & Findell, K. L. (2012). Scaling in surface hydrology: Progress and challenges. *Journal of Contemporary Water Research & Education*, *147*(1), 28–40.

Graeff, T., Zehe, E., Reusser, D., Lück, E., Schröder, B., Wenk, G., et al. (2009). Process identification through rejection of model structures in a mid-mountainous rural catchment: Observations of rainfall-runoff response, geophysical conditions and model inter-comparison. *Hydrological Processes*, *23*(5), 702–718. https://doi.org/10.1002/hyp.7171

Hawdon, A., McJannet, D., & Wallace, J. (2014). Calibration and correction procedures for cosmic-ray neutron soil moisture probes located across Australia. *Water Resources Research*, *50*, 5029–5043. https://doi.org/10.1002/2013WR015138

Heidbüchel, I., Güntner, A., & Blume, T. (2016). Use of cosmic-ray neutron sensors for soil moisture monitoring in forests. *Hydrology and Earth System Sciences*, *20*, 1269–1288.

Houben, L. J. M. (1994). *Structural design of pavements. Pt. 4. Design of concrete pavements: Dictaat Behorende Bij College CT4860*. Delft, the Netherlands: TU Delft.

Jun, I., Mitrofanov, I., Litvak, M. L., Sanin, A. B., Kim, W., Behar, A., et al. (2013). Neutron background environment measured by the mars science laboratory's dynamic albedo of neutrons instrument during the first 100 sols. *Journal of Geophysical Research: Planets*, *118*, 2400–2412. https://doi.org/10.1002/2013JE004510

Kerr, Y. H. (2007). Soil moisture from space: Where are we? *Hydrogeology Journal*, *15*(1), 117–120. https://doi.org/10.1007/s10040-006-0095-3

Kögler, S., Wagner, N., Zacharias, S., & Wollschläger, U. (2013). *Characterization of reference materials for an economic calibration approach for low-cost soil moisture sensors*. Paper presented at the Proceedings of ISEMA 2013 (pp. 442–448).

Köhli, M., Schrön, M., & Schmidt, U. (2018). Response functions for detectors in cosmic ray neutron sensing. *Nuclear Instruments and Methods in Physics Research Section A: Accelerators, Spectrometers, Detectors and Associated Equipment*, *902*, 184–189. https://doi.org/10.1016/j.nima.2018.06.052

Köhli, M., Schrön, M., Zreda, M., Schmidt, U., Dietrich, P., & Zacharias, S. (2015). Footprint characteristics revised for field-scale soil moisture monitoring with cosmic-ray neutrons. *Water Resources Research*, *51*, 5772–5790. https://doi.org/10.1002/2015WR017169

Liu, Y. Y., Parinussa, R., Dorigo, W. A., De Jeu, R. A., Wagner, W., Van Dijk, A., et al. (2011). Developing an improved soil moisture dataset by blending passive and active microwave satellite-based retrievals. *Hydrology and Earth System Sciences*, *15*(2), 425–436.

Martini, E., Wollschläger, U., Kögler, S., Behrens, T., Dietrich, P., Reinstorf, F., et al. (2015). Spatial and temporal dynamics of hillslope-scale soil moisture patterns: Characteristic states and transition mechanisms. *Vadose Zone Journal*, *14*(4).

McConn, R. J., Gesh, C. J., Pagh, R. T., Rucker, R. A., & Williams, R., III (2011). *Compendium of material composition data for radiation transport modeling* (Technical report). Richland, WA: Pacific Northwest National Laboratory.

McJannet, D., Franz, T., Hawdon, A., Boadle, D., Baker, B., Almeida, A., et al. (2014). Field testing of the universal calibration function for determination of soil moisture with cosmic-ray neutrons. *Water Resources Research*, *50*, 5235–5248. https://doi.org/10.1002/2014WR015513

McJannet, D., Hawdon, A., Baker, B., Renzullo, L., & Searle, R. (2017). Multiscale soil moisture estimates using static and roving cosmic-ray soil moisture sensors. *Hydrology and Earth System Sciences*, *21*(12), 6049–6067. https://doi.org/10.5194/hess-21-6049-2017

Montzka, C., Bogena, H., Zreda, M., Monerris, A., Morrison, R., Muddu, S., et al. (2017). Validation of spaceborne and modelled surface soil moisture products with cosmic-ray neutron probes. *Remote Sensing*, *9*(2). https://doi.org/10.3390/rs9020103

Ochsner, T. E., Cosh, M. H., Cuenca, R. H., Dorigo, W. A., Draper, C. S., Hagimoto, Y., et al. (2013). State of the art in large-scale soil moisture monitoring. *Soil Science Society of America Journal*, *77*(6), 1888–1919.

Persons, T., & Aloise, G. (2011). *Neutron detectors: Alternatives to using helium-3* (United States Government Accountability Office GAO-11–753).

Peters-Lidard, C. D., Clark, M., Samaniego, L., Verhoest, N. E. C., van Emmerik, T., Uijlenhoet, R., et al. (2017). Scaling, similarity, and the fourth paradigm for hydrology. *Hydrology and Earth System Sciences Discussions*, *21*, 3701–3713. https://doi.org/10.5194/hess-2016-695

Peterson, A. M., Helgason, W. D., & Ireson, A. M. (2016). Estimating field-scale root zone soil moisture using the cosmic-ray neutron probe. *Hydrology and Earth System Sciences*, *20*(4), 1373.

Robinson, D., Campbell, C., Hopmans, J., Hornbuckle, B., Jones, S. B., Knight, R., et al. (2008). Soil moisture measurement for ecological and hydrological watershed-scale observatories: A review. *Vadose Zone Journal*, *7*(1), 358–389.

Rosolem, R., Shuttleworth, W. J., Zreda, M., Franz, T. E., Zeng, X., & Kurc, S. A. (2013). The effect of atmospheric water vapor on neutron count in the cosmic-ray soil moisture observing system. *Journal of Hydrometeorology*, *14*(5), 1659–1671. https://doi.org/10.1175/JHM-D-12-0120.1

Roth, K., Schulin, R., Flühler, H., & Attinger, W. (1990). Calibration of time domain reflectometry for water content measurement using a composite dielectric approach. *Water Resources Research*, *26*(10), 2267–2273. https://doi.org/10.1029/WR026i010p02267

Saarenketo, T., & Scullion, T. (2000). Road evaluation with ground penetrating radar. *Journal of Applied Geophysics*, *43*(2), 119–138. https://doi.org/10.1016/S0926-9851(99)00052-X

Schattan, P., Baroni, G., Oswald, S. E., Schöber, J., Fey, C., Kormann, C., et al. (2017). Continuous monitoring of snowpack dynamics in alpine terrain by aboveground neutron sensing. *Water Resources Research*, *53*, 3615–3634. https://doi.org/10.1002/2016WR020234

Schrön, M. (2017). *Cosmic-ray neutron sensing and its applications to soil and land surface hydrology* (PhD thesis). Potsdam, Germany: University of Potsdam.

Schrön, M., Köhli, M., Scheiffele, L., Iwema, J., Bogena, H. R., Lv, L., et al. (2017). Improving calibration and validation of cosmic-ray neutron sensors in the light of spatial sensitivity. *Hydrology and Earth System Sciences*, *21*(10), 5009–5030. https://doi.org/10.5194/hess-21-5009-2017

Schrön, M., Zacharias, S., Köhli, M., Weimar, J., & Dietrich, P. (2015). Monitoring environmental water with ground albedo neutrons and correction for incoming cosmic rays with neutron monitor data. *PoS Proceedings of Science*, *231*, 101–104. https://doi.org/10.22323/1.236.0231

Schrön, M., Zacharias, S., Womack, G., Köhli, M., Desilets, D., Oswald, S. E., et al. (2018). Intercomparison of cosmic-ray neutron sensors and water balance monitoring in an urban environment. *Geoscientific Instrumentation, Methods and Data Systems*, *7*(1), 83–99. https://doi.org/10.5194/gi-7-83-2018

Schröter, I., Paasche, H., Dietrich, P., & Wollschläger, U. (2015). Estimation of catchment-scale soil moisture patterns based on terrain data and sparse TDR measurements using a fuzzy c-means clustering approach. *Vadose Zone Journal*, *14*(11). https://doi.org/10.2136/vzj2015.01.0008

Schröter, I., Paasche, H., Doktor, D., Xu, X., Dietrich, P., & Wollschläger, U. (2017). Estimating soil moisture patterns with remote sensing and terrain data at the small catchment scale. *Vadose Zone Journal*, *16*(10). https://doi.org/10.2136/vzj2017.01.0012

Schulz, K., Seppelt, R., Zehe, E., Vogel, H., & Attinger, S. (2006). Importance of spatial structures in advancing hydrological sciences. *Water Resources Research*, *42*, W03S03. https://doi.org/10.1029/2005WR004301

Seneviratne, S. I., Corti, T., Davin, E. L., Hirschi, M., Jaeger, E. B., Lehner, I., et al. (2010). Investigating soil moisture–climate interactions in a changing climate: A review. *Earth-Science Reviews*, *99*(3), 125–161.

Silvestro, F., Gabellani, S., Rudari, R., Delogu, F., Laiolo, P., & Boni, G. (2015). Uncertainty reduction and parameter estimation of a distributed hydrological model with ground and remote-sensing data. *Hydrology and Earth System Sciences*, *19*(4), 1727.

Stroup-Gardiner, M., & Brown, E. R. (2000). *Segregation in hot-mix asphalt pavements* (441). Transportation Research Board.

Vaz, C. M., Jones, S., Meding, M., & Tuller, M. (2013). Evaluation of standard calibration functions for eight electromagnetic soil moisture sensors. *Vadose Zone Journal*, *12*(2).

Vereecken, H., Huisman, J.-A., Hendricks Franssen, H.-J., Brüggemann, N., Bogena, H. R., Kollet, S., et al. (2015). Soil hydrology: Recent methodological advances, challenges, and perspectives. *Water Resources Research*, *51*, 2616–2633. https://doi.org/10.1002/2014WR016852

Wagner, W., Verhoest, N., Ludwig, R., & Tedesco, M. (2009). Editorial: Remote sensing in hydrological sciences. *Hydrology and Earth System Sciences*, *13*(6), 813–817.

Wang, L., & Qu, J. J. (2009). Satellite remote sensing applications for surface soil moisture monitoring: A review. *Frontiers of Earth Science in China*, *3*(2), 237–247.

Webster, R., & Oliver, M. A. (1992). Sample adequately to estimate variograms of soil properties. *European Journal of Soil Science*, *43*(1), 177–192.

Western, A. W., Grayson, R. B., & Blöschl, G. (2002). Scaling of soil moisture: A hydrologic perspective. *Annual Review of Earth and Planetary Sciences*, *30*(1), 149–180.

Wolf, B., Chwala, C., Fersch, B., Garvelmann, J., Junkermann, W., Zeeman, M., et al. (2016). The SCALEX campaign: Scale-crossing land-surface and boundary layer processes in the TERENO-preAlpine Observatory. *Bulletin of the American Meteorological Society*, *98*, 1217–1234.

Wollschläger, U., Attinger, S., Borchardt, D., Brauns, M., Cuntz, M., Dietrich, P., et al. (2016). The Bode hydrological observatory: A platform for integrated, interdisciplinary hydro-ecological research within the TERENO Harz/Central German Lowland Observatory. *Environmental Earth Sciences*, *76*(1), 29. https://doi.org/10.1007/s12665-016-6327-5

Wood, E. F., Roundy, J. K., Troy, T. J., van Beek, L., Bierkens, M. F., Blyth, E., et al. (2011). Hyperresolution global land surface modeling: Meeting a grand challenge for monitoring Earth's terrestrial water. *Water Resources Research*, *47*, W05301. https://doi.org/10.1029/2010WR010090

Zacharias, S., H., Bogena, L., Samaniego, M., Mauder, R., Fuß, T., Pütz, M., et al. (2011). A network of terrestrial environmental observatories in germany. *Vadose Zone Journal*, *10*(3), 955–973. https://doi.org/10.2136/vzj2010.0139

Zhu, X., Shao, M., Zeng, C., Jia, X., Huang, L., Zhang, Y., et al. (2016). Application of cosmic-ray neutron sensing to monitor soil water content in an alpine meadow ecosystem on the Northern Tibetan Plateau. *Journal of Hydrology*, *536*, 247–254.

Zink, M., Samaniego, L., Kumar, R., Thober, S., Mai, J., Schäfer, D., et al. (2016). The German drought monitor. *Environmental Research Letters*, *11*(7).

Zreda, M., Desilets, D., Ferré, T. P. A., & Scott, R. L. (2008). Measuring soil moisture content non-invasively at intermediate spatial scale using cosmic-ray neutrons. *Geophysical Research Letters*, *35*, L21402. https://doi.org/10.1029/2008GL035655

Zreda, M., Shuttleworth, W. J., Zeng, X., Zweck, C., Desilets, D., Franz, T., et al. (2012). COSMOS: The COsmic-ray Soil Moisture Observing System. *Hydrology and Earth System Sciences*, *16*(11), 4079–4099. https://doi.org/10.5194/hess-16-4079-2012